A facile controllable coating of carbonyl iron particles with poly(glycidyl methacrylate): A tool for adjusting MR response and stability properties

Martin Cvek,[a,b] Miroslav Mrlik,[a,c] Marketa Ilcikova,[c,d] Tomas Plachy,[a] Michal Sedlacik,[a] Jaroslav Mosnacek,[d] Vladimir Pavlinek,[a]*

[a] Centre of Polymer Systems, University Institute, Tomas Bata University in Zlin, Nad Ovcirnou 3685, 760 01 Zlin, Czech Republic

[b] Polymer Centre, Faculty of Technology, Tomas Bata University in Zlin, nam. T. G. Masaryka 275, 762 72 Zlin, Czech Republic

[c] Center for Advanced Materials, Qatar University, P. O. BOX 2713, Doha, Qatar

[d] Polymer Institute, Slovak Academy of Sciences, Dubravska cesta 9, 845 41 Bratislava 45, Slovakia

Keywords: magnetorheological suspension, atom transfer radical polymerization, carbonyl iron, poly(glycidyl methacrylate), core-shell, suspension stability

Abstract

This study is focused on the controllable coating of the carbonyl iron (CI) particles widely applied in magnetorheology. These particles were grafted with poly(glycidyl methacrylate) (PGMA) with narrow dispersion *via* surface-initiated atom transfer radical polymerization. Two types of core-shell particles differing in molecular weights of grafted polymer chains were synthesized. The effect of shell thickness on the thermo-oxidation stability of particles as well as the sedimentation stability of their silicone oil suspensions was evaluated. The successful coating process was confirmed by Fourier transform infrared spectroscopy and energy-dispersive spectrometry. The differences in the magnetic properties of bare and coated CI particles were clarified through vibrating magnetometry. Due to the controllable length of the PGMA grafts, the magnetic properties remain almost the same as those for bare CI. The magnetorheological (MR) behavior of silicone oil suspensions containing 60 wt.% of bare CI particles as well as PGMA-coated analogues were investigated in the presence and absence of various magnetic field strengths, demonstrating the negligible impact of surface modification on final MR performance. Thus, the grafting of the particles with PGMA negligibly affected magnetic properties but considerably enhanced thermo-oxidation and sedimentation stability. Finally, the novel tensiometric method for sedimentation stability measurements of MR suspensions was successfully implemented.

1. INTRODUCION

Magnetorheological (MR) suspensions are fluids that have their rheological behavior altered (yield stress, apparent viscosity, storage modulus) by the application of an external magnetic field [1–3]. Generally, MR suspensions consist of solid, usually micron-sized, magnetically-polarizable particles dispersed in a non-magnetic carrier liquid such as silicone or mineral oils. In the absence of an external magnetic field (off-state), particles are randomly dispersed in the carrier liquid. The MR suspension has low viscosity depending on the carrier liquid and behaves almost like a Newtonian fluid. After the application of an external field (on-state), the particles are polarized and in a fraction of a millisecond create highly-organized structures, which results in the predominance of magnetic forces over hydrodynamic ones. When the chain-like structures are formed, the viscosity and viscoelastic moduli increase by several orders of magnitude. The orientation of chain-like structures is along the magnetic field direction, and their toughness is a function of the applied magnetic field strength. This phenomenon is reversible and is called the MR effect [1–6].

Nowadays, MR suspensions are well-known and referred to as “intelligent” or “smart” materials, which play an important role in many engineering applications due to their fine-tuning material behavior. Their unique properties preferably can be used for the active control of vibrations or the transmission of torque. Typical applications include dampers [7–10], brakes [11, 12], clutches [13, 14], prosthetic devices [15] or ultrafine polishing devices [16]. Also, biomedical applications such as drug targeting [17] or hyperthermia in cancer therapy [18] have been recently studied in regard to these systems. The broad applicability of these suspensions therefore attracts both scientific and industrial interests.

Despite such braod applications, some drawbacks hinder their potential. Due to the large density difference between metal particles and carrier oils, poor sedimentation stability is a common problem [19]. Several methods can enhance sedimentation stability, including the addition of surfactant systems [20] or nano-sized particles such as fumed silica [21], organic clays [22], carbon nanotubes [23] or graphite micro-particles [24]. Although the addition of fillers can increase sedimentation stability, the off-state viscosity inevitably increases, which can be a problem in some applications. Therefore, the application of a polymer coating on the surface of the particles seems to be a wise strategy to counter this drawback [2, 25]. Various processes for the preparation of core-shell particles have been used, including dispersion polymerization, suspension polymerization or solvent evaporation. Also many polymers have been used as a shell material,, e.g., poly(methyl methacrylate) [26] or polystyrene [27], which were synthesized *via* both dispersion and suspension polymerizations. Coatings consisting of poly(vinyl butyral) [28] or polycarbonate [29] were prepared using solvent evaporation. Another approach is utilizing the vacuum plasma deposition of fluorinated substances [30]. Furthermore, electrically-conductive polymers such as polypyrrole [31] or polyaniline [3] were successfully used as non-covalently bonded shell materials for this reason. The thickness of the coating layer using suspension polymerization is 2–10 microns, while dispersion polymerization creates submicron coating layers. However, as is widely known, with the increasing thickness of polymer coating, the saturation magnetization (or magnetic susceptibility) decreases, which causes a lower yield stress generation in the on-state of MR suspensions [2]. Therefore, there is a need to precisely control the molecular weight of a grafted polymer and thus to be able to adjust the MR performance of prepared suspensions.

ATRP was introduced by Matyjaszewski et al. [32] in 1995 as one of the methods allowing for the preparation of polymers with precisely controlled molecular weight, narrow polydispersity, controlled chain composition and tailored functionalities. The ATRP system consists of alkyl halide as an initator, metal halide as a catalyst and a ligand complexing the metal halide catalyst and thus improving its solubility in a polymerization mixture and fine tuning its catalytic efficiency. ATRP can be applied to a wide range of vinyl monomers at relatively mild conditions at elevated temperatures [33, 34] or at room temperature under UV-VIS irradiation [35]. So far, only two polymers poly(butyl acrylate) [25] and poly(2-fluorostyrene) [34] with molecular weights above 15,000 g·mol^{-1} were grafted using surface-initiated ATRP (SI-ATRP) in order to prepare core-shell CI-polymer particles for MR suspensions. However, magnetic properties were significantly suppressed in the mentioned studies due to the thick shells of the high molecular weight polymer chains.

Therefore, this study was aimed at using SI-ATRP for the preparation of CI particles grafted with poly(glycidyl methacrylate) (CI-PGMA) of short chain-lengths in order to investigate whether such short polymer chains can provide sufficient sedimentation and thermo-oxidation stability while not affecting their good magnetic properties, characteristics necessary for many industrial applications.

2. EXPERIMENTAL

2.1 Materials

The CI powder (SL grade) used throughout this work is a commercial product of BASF Corporation (Germany). The chemical composition of CI, as given by the manufacturer, is a minimum 99.5 % pure iron. Glycidyl methacrylate (GMA, 97 %) was purchased from Sigma Aldrich (USA), and before use it was purified by passing it through a basic alumina in order to

remove a stabilizer. (3-Aminopropyl) triethoxysilane (APTES, ≥ 98 %) was used as a coupling agent between the CI particles and the difunctional initiator α-bromoisobutyryl bromide (BiBB, 98 %). Ethyl α-bromoisobutyrate (EBiB, 98 %) was used as a sacrificial initiator. BiBB, APTES, EBiB and other chemicals such as triethylamine (Et_3N, ≥ 99 %), *N,N,N′,N′′,N′′*-pentamethyldiethylenetriamine (PMDETA, ≥ 99 %), copper bromide (CuBr, ≥ 99%), anisole (99 %), and aluminum oxide (neural, Brockmann I), were produced by Sigma Aldrich (USA) and used as received. Silicone oil used for the preparation of MR suspensions was Lukosiol M200 (Chemical Works Kolín, Czech Republic; dynamic viscosity of 197 mPa·s, density of 0.97 g·cm^{-3}). Solvents and purification agents, namely tetrahydrofuran (THF, p.a.), acetone (p.a.), ethanol (absolute anhydrous, p.a.), toluene (p.a.), and hydrochlorid acid (HCl, 35 %, p.a.) were obtained from Penta Labs (Czech Republic).

2.2 Synthesis

Surface activation and functionalization of CI microparticles.

The fundamental procedure of chemical activation and functionalization of CI was inspired by Belyavskii et al. [36] and was also successfully used by Mrlik et al. [37]. The bulk of the CI powder (100 g) was placed into a beaker and treated with 250 mL of 0.5M HCl for 10 minutes in order to attain reactive hydroxyl groups on the CI particle surface. Acid-treated CI powder was rinsed with distilled water, ethanol, and acetone using a decantation method with a magnet at the bottom of the beaker. Finally, the powder was dried for 3 hours at 60 °C under 200 mbar in order to remove residual acetone. Surface-activated dry CI powder (90 g) was weighted into a 500 mL three-neck flask and dispersed in 300 mL of a non-polar solvent, toluene. The flask was equipped with a mechanical stirrer, a reflux condenser and a thermometer. Then, 10 mL of

APTES as a coupling agent was added, and the formed suspension was agitated under 250 rpm and refluxed for 6 hours at 110 °C. After the reaction, functionalized CI particles were thoroughly washed with toluene, ethanol, and acetone, and dried for 24 hours under 200 mbar.

Immobilization of initiator.

The immobilization of the ATRP initiator BiBB was performed in the presence of dried THF (Scheme 1) as follows: 40 g of CI particles modified with an APTES silane agent (CI-NH_2) were added into a Schlenk flask (SF), and the space of the flask was evacuated for 30 minutes. Then, 50 mL of dried THF was distilled and moved to the SF under argon atmosphere. After that, 16 mL of Et_3N were transferred into the SF. Finally, 8 mL of BiBB were added dropwise into the mixture, and the whole content of the SF was cooled down and kept in the ice bath for 3 hours. Subsequently, the mixture was stirred overnight. Then, the initiator-treated CI particles (CI-Br) were rinsed with acetone and dried for 24 hours at 60 °C under 200 mbar.

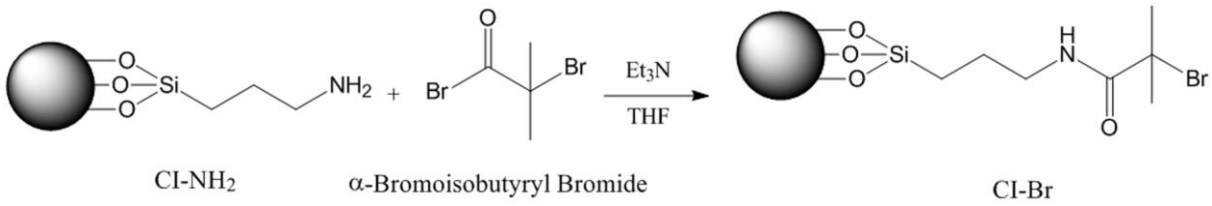

CI-NH_2 α-Bromoisobutyryl Bromide CI-Br

Scheme 1. Attachment of the initiator onto the surface of CI particles.

Surface-initiated polymerization from CI-Br particles.

In this step, 10 g of CI-Br particles were placed into SF, evacuated several times and then backfilled with argon. Then, GMA (20 mL; 0.1466 mol), PMDETA (0.1530 mL; 0.733 mmol), EBiB (0.1076 mL; 0.733 mmol) and anisole (20 mL; 0.1840 mol), were injected into the SF.

Several freeze-pump-thaw cycles with liquid nitrogen were performed to eliminate residual oxygen from the polymerization mixture, and finally the SF was filled with argon. The polymerization was initiated by the addition of a CuBr catalyst (0.1052 g; 0.733 mmol) into a polymerization mixture and placing the reaction flask into an oil bath pre-heated to 50 °C. The reaction mixture was stirred at 175 rpm for 2 hours, and then the reaction was stopped by opening the flask. Scheme 2 illustrates the described SI-ATRP approach.

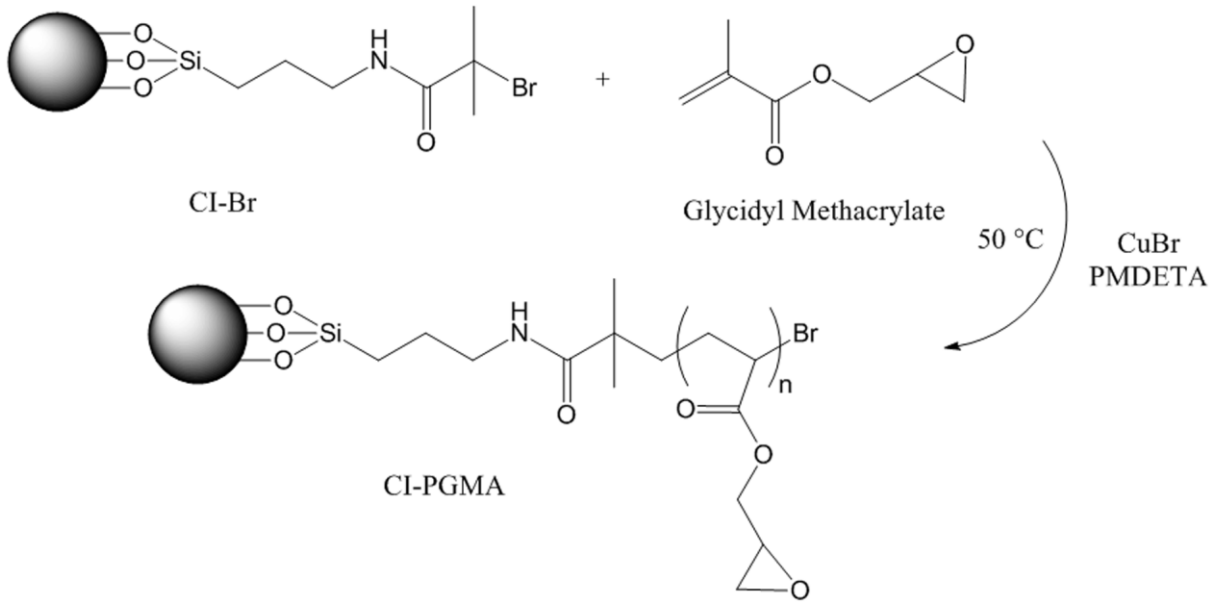

Scheme 2. Grafting of CI-Br particles with PGMA using the SI-ATRP.

CI particles grafted with higher molecular weight PGMA were synthesized in the same manner but with a higher GMA:initiator molar ratio. The amounts of monomer and solvent in this case were as follows: GMA (30 mL; 0.2199 mol) and anisole (30 mL; 0.2760 mol). The PGMA-

grafted core-shell structured particles were purified by washing with THF and acetone several times before being dried overnight at 60 °C.

2.3 General characterization

Monomer conversion was determined by ^{1}H NMR with a 400 MHz VNMRS Varian NMR spectrometer (Varian Inc. since 1999 part of Agilent, Japan) equipped with a 5 mm 1H–19F/15N–31P PFG AutoX DB NB probe at 25 °C. Deuterated chloroform ($CDCl_3$) was used as a solvent. For NMR measurement, a sample (green polymer solution) taken after 2 hours of polymerization was passed through aluminum oxide (neutral), absorbent cotton and a microfilter in order to remove the copper catalyst and CI-PGMA particles, and the colorless filtrate was supplemented by $CDCl_3$.

GPC PL-GPC220 (Agilent, Japan) was employed to determine the relative molecular weight of the polymer samples as well as the distribution of molecular weights during the polymerization. THF was used as an eluent (mobile phase) at a flow rate of 1.0 mL·min^{-1}. The polystyrene was used as a standard to calibrate the GPC, and anisole was used as an internal standard to correct any fluctuations in THF flow rate. The sample was mixed with THF, then purified in the same manner as for the ^{1}H NMR measurement and injected into a GPC column heated to 30 °C.

Morphologies of bare CI and the prepared CI-PGMA particles were examined using scanning electron microscopy (SEM; Tescan Vega II LMU, Czech Republic) with employed 5 – 10 kV of accelerating voltage. A secondary electron (SE) detector was used due to its higher depth of field. A Tescan Vega II LMU is equipped with an energy-dispersive spectroscope (EDS), which provided a surface elemental analysis of the studied particles.

Fourier transform infrared (FTIR) spectra were obtained from a Nicolet FTIR spectrometer (Nicolet 6700, USA) equipped with an ATR accessory in order to prove the success of the ATRP coating process. The measurement was performed at laboratory temperature using a Germanium crystal in the region of 4000 – 500 cm^{-1}.

The magnetic properties of the CI and CI-PGMA powders were characterized by vibrating sample magnetometry (VSM; 7407, Lakeshore, USA). Approximately 200 – 300 mg of the sample was subjected to a magnetic field in the range of ±780 $kA \cdot m^{-1}$ at laboratory temperature.

Thermo-oxidative stability, an important characteristic of the MR particles, was investigated with the help of a thermogravimetric analysis (TGA; TA Instruments Q500, USA) under air atmosphere at a heating rate of 10 $K \cdot min^{-1}$. The weight gain of the samples was observed during all TGA measurements, indicating ongoing chemical reactions. The weight gain was further plotted as a function of temperature.

2.4 Suspension preparation and rheological measurements

Three variants of MR suspensions with a 60 wt.% particle concentration in silicone oil were prepared. The first suspension was based on bare CI particles, while the second and third suspensions contained CI-PGMA particles grafted with PGMA of different molecular weights.

The rheological properties of MR suspensions in oscillatory shear mode in the absence as well as in the presence of various magnetic field strengths were experimentally studied. Measurements were carried out with the Physica MCR502 (Anton Paar GmbH, Austria) rheometer equipped with a magnetic cell (Physica MRD 170+H-PTD200) using a parallel plate (PP20/MRD/TI) geometry with a diameter of 20 mm. A gap of 0.5 mm was maintained between the plates, and a 0.2 mL sample of the MR suspension was placed between them.

The small-strain oscillatory tests were carried out through strain sweeps and frequency sweeps. The linear viscoelasticity region (LVR) was found through a storage modulus, G', measurement as a function of strain, γ. The used strain range was (10^{-3} – 10^{1} %) at a fixed frequency of 1 Hz under different magnetic field strengths. Then, frequency sweeps were performed in a range of frequencies (0.1 – 10 Hz) at a constant amplitude strain (obtained from LVR investigation). Prior to each on-state measurement, field-induced structures were agitated by continuous shearing (shear rate 50 s^{-1}) for one minute. Then, the new magnetic field strength was imposed (0 – 438 $kA \cdot m^{-1}$). The temperature was maintained at 25 °C with a closed-cycle cooling system (Julabo FS18, Germany). To avoid sedimentation, the tests were started as soon as the thoroughly-mixed suspension was injected into the measuring system.

2.5 Sedimentation stability measurements

The sedimentation stability of MR suspensions based on CI and both variants of CI-PGMA particles was determined by a Tensiometer Krüss K100 (MK2/SF/C, Hamburg, Germany) at laboratory temperature. An evaluation of sedimentation stability of MR suspensions *via* tensiometry was recently proposed by Sedlacik [38]. MR suspensions containing 10 wt.% of CI particles or their PGMA-coated analogues in silicone oil were prepared by thorough mixing followed by sonication using an ultrasound device (Sonopuls HD 2070, Bandelin electronic, Germany) for 2 minutes. The funnel-shaped measuring probe was hung up on scales and then immersed in the test suspension. The total height of the tested suspension was 45 mm, while the measuring probe was placed 20 mm under the surface. The probe captured settling particles and evaluated their weight as a function of time. The sedimentation measurements were performed for 2 hours, i.e., until a plateau in a mass increment was observed.

3. RESULTS AND DISCUSSION

3.1 CI-PGMA synthesis, ^{1}H NMR and GPC investigation

The molecular weight of a polymer coating can significantly affect the properties of MR particles. If the molecular weight is too low and thus the shell too thin, the polymer shell will not prevent CI particles from settling. On the contrary, too high of a molecular weight of a polymer coating can cause an undesirably large increase in off-state viscosity [25]. Therefore, CI particles coated with PGMA of two different molecular weights were prepared. The syntheses of CI-PGMA particles were performed at 50 °C *via* SI-ATRP using EBiB as a macroinitiator, CuBr as a catalyst and PMDETA as a ligand in molar ratios [GMA]:[EBiB]:[CuBr]:[PMDETA] = [200]:[1]:[1]:[1] and [300]:[1]:[1]:[1]. The conversion value expresses the percentage of monomer units built into polymer chains and was determined by ^{1}H NMR. The weight-average molecular weight ($\overline{M}_W$) and number-average molecular weight ($\overline{M}_n$) of PGMA were determined by GPC analysis based on free PGMA chains grown from a free sacrificial initiator, under the assumption of the similar growth of polymers from free and bond initiator. The results are summarized in Table 1. A relatively narrow polydispersity in both polymerizations implies that the ATRP was well controlled and the thickness of the PGMA coating on the CI particles could be expected to be uniform.

Table 1. Results of SI-ATRP of PGMA performed at 50 °C.

Sample code	GMA	Time	Conversion[a]	$\overline{M}_W$	$\overline{M}_n$	PDI

	[mL]	[min]	[%]	[g·mol^{-1}]	[g·mol^{-1}]	[-]
CI-PGMA-1	20	120	87.0	6 600	5 000	1.32
CI-PGMA-2	30	120	88.5	12 500	9 700	1.29

[a]Based on ^{1}H NMR spectra

3.2 Scanning electron microscopy

SEM micrographs of original CI particles and prepared CI-PGMA particles are displayed in Figure 1. The SEM analysis confirmed that bare CI particles as well as CI-PGMA particles have a spherical shape. However, the presence of the rod-like particles in the sample of bare CI, probably as an incomplete product of CI synthesis, was also observed (Figure 1a). Modification affected the particle morphology; the surface of bare CI particles is quite smooth, whereas the surface of coated CI particles is rougher, which indicates the presence of grafted PGMA polymer chains (Figure 1b).

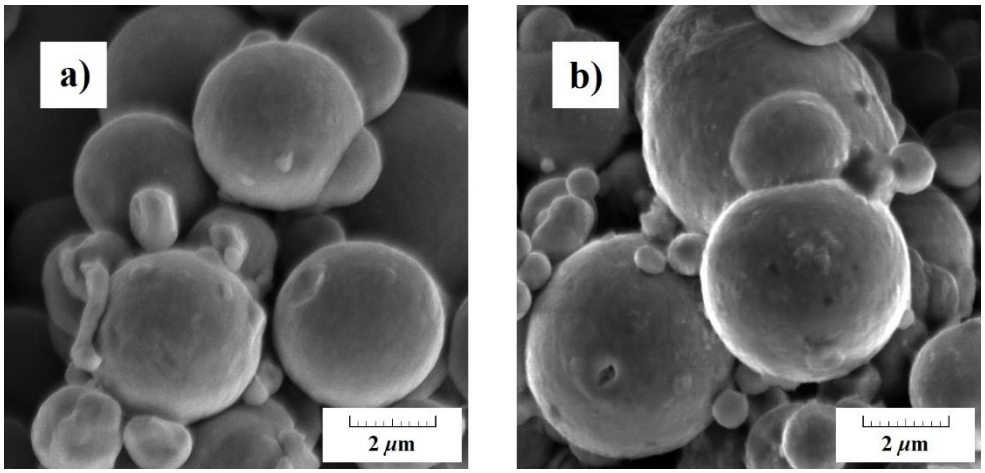

Figure 1. SEM images of bare CI particles (a) and CI-PGMA-1 particles (b).

3.3 Energy dispersive spectroscopy

Figure 2 shows a representative EDS spectrum of bare CI particles. As expected, the examined sample is almost pure iron with some carbon contained as a small impurity present in the CI after fabrication. The EDS spectrum of PGMA-coated CI particles is illustrated in Figure 3. The most represented element is iron. The second most frequent element is carbon, which is partly from CI impurity and partly from the individual components (the coupling agent, residue of initiator, and the PGMA chain) constituting the whole graft (Table 2). The EDS analysis also revealed silicon atoms, which originate from the APTES coupling agent. Here, the presence of oxygen can also be seen, which is a signal from the coupling agent as well as from the PGMA polymer chain. However, its Kα emission was overlapped in the low energy shoulder of the broad iron L emission peak (the inset of Figure 3). In general, the EDS analysis proved the presence of expected elements indicative of a successful coating process. The content of each element occurring in the samples expressed as a weight percentage is summarized in Table 2.

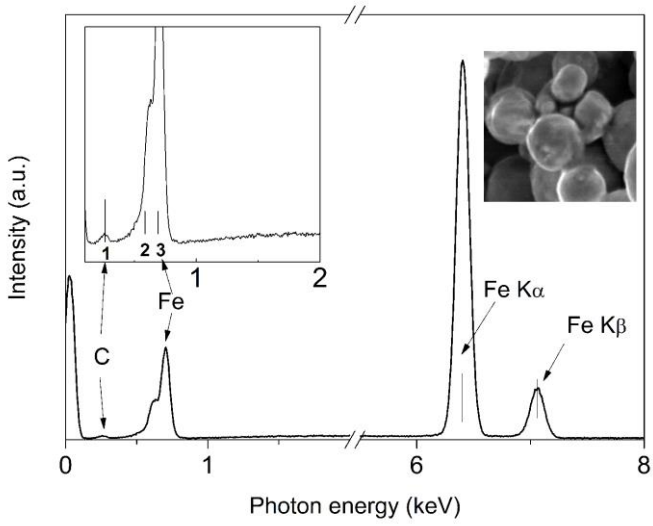

Figure 2. The EDS spectrum of the surface of the bare CI particles, with magnified details in graph inset: 1 – C Kα line, 2 and 3 – Fe L lines. The inset image shows the place fromwhere the spectrum was collected.

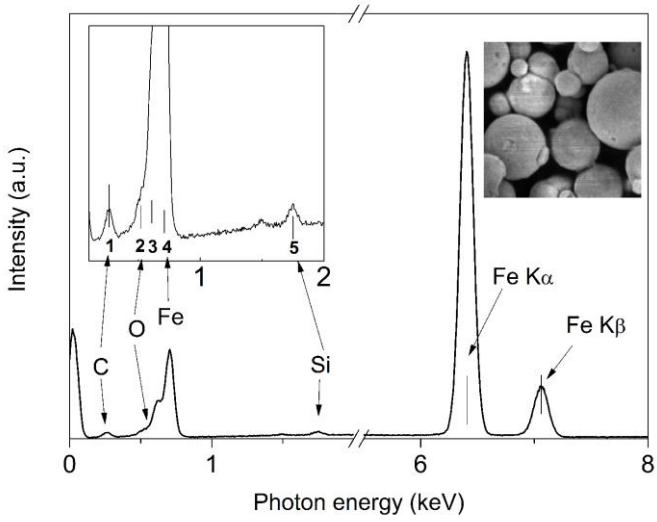

Figure 3. The EDS spectrum of the surface of the CI-PGMA-1 particles, with magnified details in the graph inset: 1 – C Kα line, 2 – O Kα line, 3 and 4 – Fe L lines, 5 – Si Kα line. The inset image shows the place from where the spectrum was collected.

Table 2. Results of EDS elemental analysis.

Element	Atomic%	
	bare CI particles	CI-PGMA-1 particles
Fe	82.1	65.7
C	17.9	27.8
O	0.0	5.7
Si	0.0	0.8
Total	100.0	100.0

3.4 Fourier transform infrared spectroscopy

FTIR spectral curves of bare CI particles and PGMA-coated CI particles were compared. Figure 4 illustrates the differences in wavenumbers of individual spectra. In the spectrum of the CI-PGMA composite particles, the appearance of a characteristic peak around 1,714 cm^{-1} reflects the stretching vibration of the –C=O carbonyl group. Vibrations at 1,305 cm^{-1} indicate a C–O–C bond of methacrylate. Sharp peaks at 904 cm^{-1} and 815 cm^{-1} are an oxirane ring contraction vibration and an unsymmetrical expansion [39, 40]. Hence, FTIR spectroscopy was another method proving the successful coating of the CI particles.

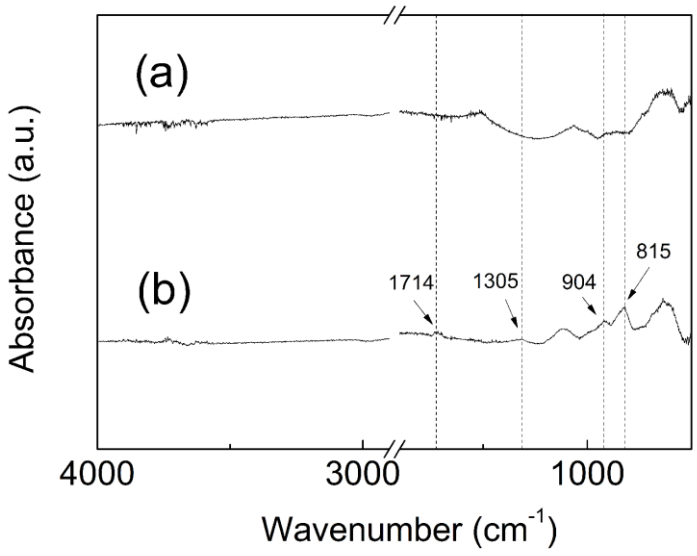

Figure 4. FTIR spectra of (a) bare CI particles, and (b) PGMA-coated CI particles.

3.5 Magnetic properties

VSM measurements were performed in order to determine the magnetic properties of bare CI as well as coated CI-PGMA particles. The magnetization curves for bare CI particles and both variants of PGMA-coated CI particles exhibit a similar character, as presented in Figure 5. True

saturation magnetization of the particles was not reached due to the insufficient intensity of the external magnetic field. According to de Vicente et al. [41], the saturation magnetization of the CI powder can be reached at a magnetic field strength of 1,360 $kA \cdot m^{-1}$. The actual measured magnetization (obtained for a magnetic field strength of 780 $kA \cdot m^{-1}$) of utilized bare CI particles was 178.79 $emu \cdot g^{-1}$. For coated particles, the magnetizations at the same magnetic field strength were 171.77 $emu \cdot g^{-1}$ and 169.32 $emu \cdot g^{-1}$, which is only a 3.9 % and 5.3 % decrease, respectively, compared to bare CI particles. A decrease in observed magnetization was expected due to the non-magnetic polymer shell, but the decrease is negligible. Therefore, the impact on the MR effect should not be severe. In 2014, Kim et al. [4] fabricated CI-PGMA particles by cross-linking PGMA with ethylene glycol dimethacrylate, and quite a large magnetization decrease at a comparable magnetic field strength was reported, i.e., from 175 $emu \cdot g^{-1}$ to 85 $emu \cdot g^{-1}$, which represents a 51.4 % decrease.

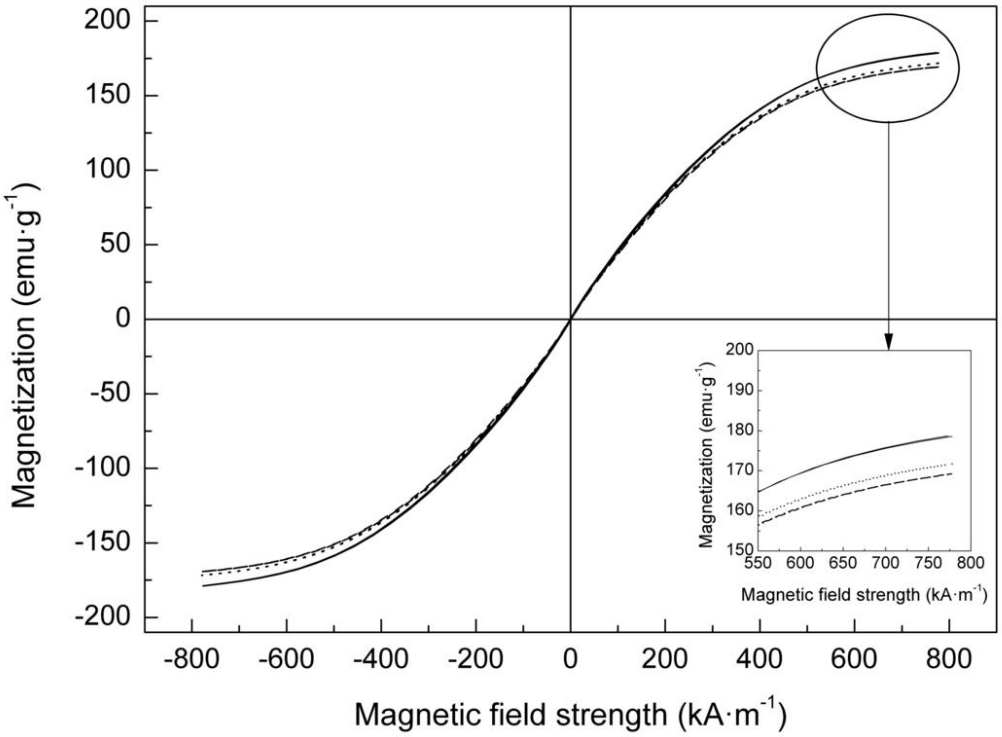

Figure 5. Magnetization curves of (–) bare CI particles, (····) CI-PGMA-1 particles, and (- - -) CI-PGMA-2 particles.

Table 3. Results of VSM measurement

Sample code	Magnetization at 780 kA·m^{-1} [emu·g^{-1}]	Coercivity [kA·m^{-1}]
CI	178.79	0.95
CI-PGMA-1	171.77	0.91
CI-PGMA-2	169.32	0.94

The other monitored parameter was coercivity. The lower it is, the better the dynamic of the demagnetization of the particles. VSM measurements show that the polymer coating hardly affected the coercivity, which is also a positive outcome (Table 3). The measured coercivity of bare CI particles was 0.95 $kA \cdot m^{-1}$, while 0.91 $kA \cdot m^{-1}$ for CI-PGMA-1 particles, and 0.94 $kA \cdot m^{-1}$ for CI-PGMA-2 particles, respectively. The retained high values of magnetization and unaltered coercivity make the prepared CI-PGMA particles promising candidates for the effective utilization of their MR suspensions in practical applications.

3.6 Thermo-oxidative stability

The weight gain was plotted as a function of temperature as shown in Figure 6. Clearly, such a weight gain is the result of iron oxide formation. Iron powder takes up to 40 wt.% of oxygen and forms oxides as follows: FeO, Fe_3O_4 and finally Fe_2O_3 [42]. The figure shows that the reaction requires an exceptionally-wide temperature range to achieve full conversion. The weight of bare CI particles started to increase at lower temperatures compared to core-shell structured CI particles. As expected, the PGMA polymer coating on the surface of CI particles leads to considerable thermo-oxidative resistance enhancement. The first weight changes of bare CI particles were observed at temperatures around 200 °C. Both variants of PGMA-coated CI particles were thermally stable up to 300 °C. A significant increase in the weight of uncoated CI particles occurs at temperatures around 400 °C, while a similar sharp weight gain due to severe oxidation is shifted to temperatures above 500 °C for both coated CI particle variants.

Figure 6 also demonstrates that the polymer-coated CI particles thermally decompose and the inner iron core is simultaneously oxidized during heating. If the polymer decomposed first, the weight decrease would be displayed on the thermogram, so the reactions probably took place concurrently. A small weight decrease occurred around 650 °C in both variants of coated

particles. This could be due to some absorbed gases on the particle surface. A grafted polymer coating thus provides a protective over-layer on the CI particles, which shifted the oxidation process to higher temperatures; however, the doubling of its molecular weight further contributes to only a slight improvement in thermo-oxidative resistance.

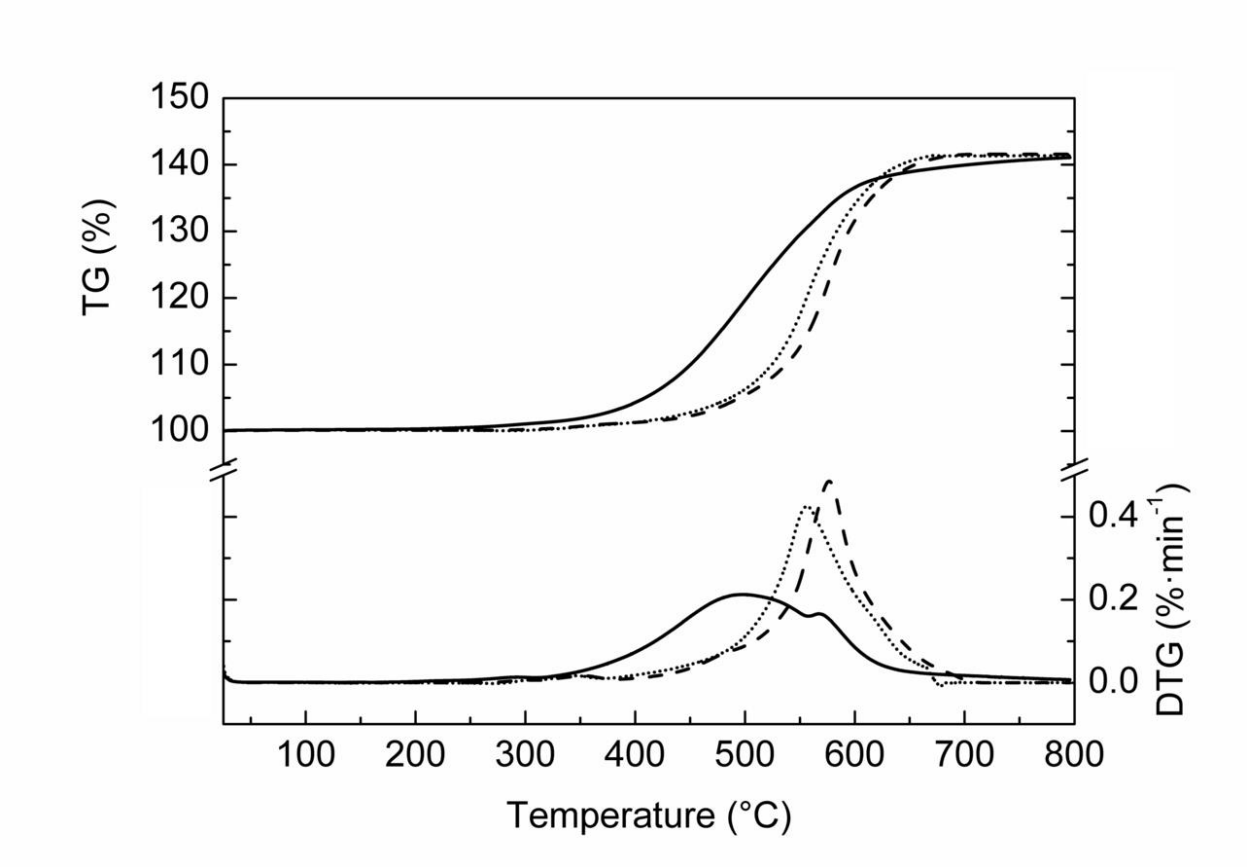

Figure 6. TG and DTG curves of bare CI particles (–), CI-PGMA-1 particles (····), and CI-PGMA-2 particles (- - -) in the atmosphere.

3.7 Rheological properties in oscillatory mode

Oscillatory tests at sufficiently low deformations do not destroy the structure [43], and therefore they were established as a suitable tool to evaluate the behavior of MR suspensions at dynamic strain. The LVR was determined in an amplitude sweep test, which is necessary because the values of G' and loss modulus, G'', have a physical meaning only when the internal structures are not broken [44]. Therefore, the dependence of G' and G'' on γ for oscillatory shear flow was investigated. The position of LVR changes depending on the strength of the applied magnetic field [6], but the change was negligible in our measurements. The apparent decrease of G' appeared at a 0.04 % amplitude strain for a 60 wt.% MR suspension based on bare CI as well as on both variants of CI-PGMA particles. All studied MR suspensions exhibited G'' larger than G' within the whole strain range in the absence of a magnetic field, which indicates a liquid-like behavior. After the application of the magnetic field, the MR suspensions exhibited solid-like behavior due to a chain-like structure formation, and G' became higher than G''. However, G'' exhibited non-zero values, which is according to Ramos et al. [44] due to the existence of free chains with one or two ends not connected to the surface of the geometry.

The effect of particle surface modification on the critical strain, γ_C, of MR suspensions was evaluated. Critical strain is defined as the value of the strain where G' and G'' moduli are equal, which represents the transition between the viscoelastic-solid at low strain and the viscoelastic-liquid at high strain values. Moreover, this parameter is responsible for a competition between magnetic forces and hydrodynamic forces [43]. It was observed that a higher magnetic field strength leads to a higher value of γ_C, because a larger magnetic field is able to retain a solid structure to higher strains. MR suspensions containing modified particles exhibited lower values of critical strain at all magnetic field strengths compared to the suspension of bare CI particles. This effect was more obvious in the suspension based on CI-PGMA-2 particles.

The determined strain amplitude of the LVR position was maintained within the range of frequencies (0.1 – 10 Hz), and the viscoelastic moduli were evaluated. In all measurements, the viscoelastic moduli in the off-state exhibit a slow but gradual increase over a wide range of frequencies. On the other hand, in the on-state, the G' and G'' were almost independent in the measured frequency range. An applied magnetic field strength caused increases of G' as well as G'' for all prepared suspensions. Comparing suspensions off-state with on-state at 438 $kA \cdot m^{-1}$, G' increased by a factor of 10^5, whereas G'' increased by a factor of 10^4. This phenomenon is similar for all prepared suspensions.

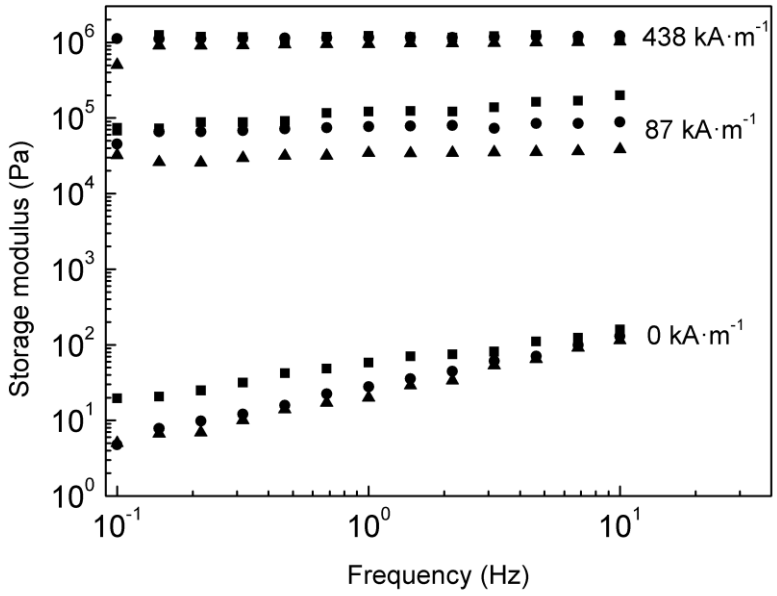

Figure 7. A comparison of storage modulus, G', as a function of frequency for suspensions containing 60 wt.% of bare CI particles (■), CI-PGMA-1 particles (●), and CI-PGMA-2 particles (▲) at various magnetic field strengths.

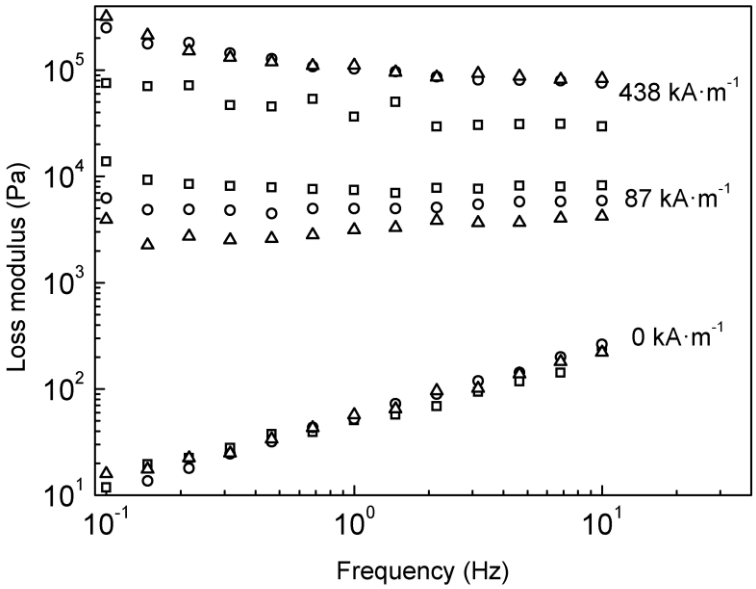

Figure 8. A comparison of loss modulus, G'', as a function of frequency for suspensions containing 60 wt.% of bare CI particles (□), CI-PGMA-1 particles (○), and CI-PGMA-2 particles (Δ) at various magnetic field strengths.

Figure 7 compares G', which is related to chain toughness depending on frequency at certain magnetic field strengths. G' exhibits similar values for each suspension at the same magnetic field strength with only slight deviations. Also values of G'' are almost identical, which demonstrates similar heat dissipation in the MR suspensions during dynamic strain (Figure 8). Frequency sweeps were analyzed at 5 different magnetic field strengths (87 kA·m^{-1}, 173 kA·m^{-1}, 262 kA m^{-1}, 351 kA·m^{-1}, and 438 kA·m^{-1}) (data not shown here) in order to determine the dynamic efficiency (e) of MR suspensions, which is defined as: $e\,(f) = (G'(H)\text{-}G'(0))/G'(0)$ and was evaluated at 1 Hz as a function of applied magnetic field strength (Figure 9). In all suspensions, dynamic efficiency generally increased with increasing magnetic field strength. At

relatively low fields (up to 173 kA·m^{-1}), values of the dynamic efficiency exhibit a sharp increase, while at higher magnetic field strengths its values started to plateau. MR suspensions of modified CI particles showed even higher values of dynamic efficiency, which is due to lower off-state storage modulus and comparable on-state modulus. In this case, the molecular weight of grafted PGMA did not have a distinct effect on dynamic efficiency, and only slight deviations between efficiencies of modified suspensions were observed.

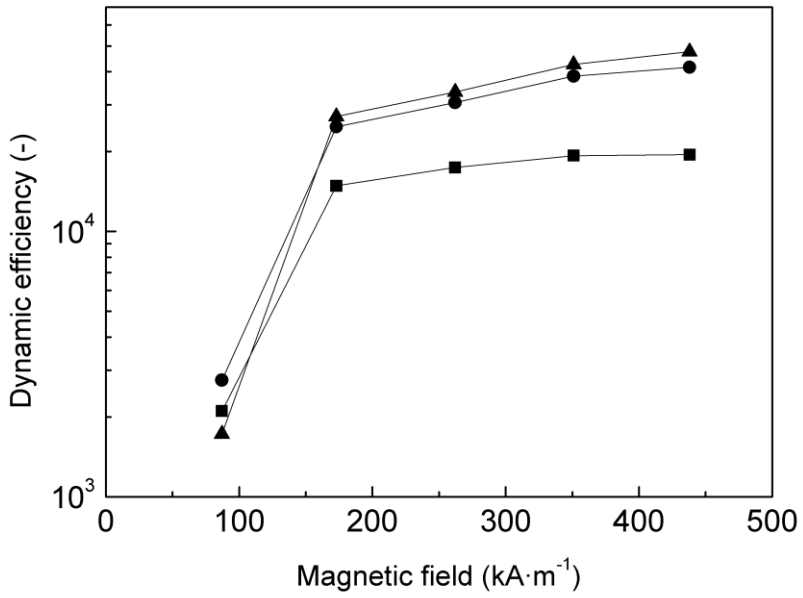

Figure 9. Dynamic efficiency as a function of magnetic field strength for MR suspensions containing 60 wt.% of bare CI particles (■), CI-PGMA-1 particles (●), and CI-PGMA-2 particles (▲).

It can be concluded that the controllably-grafted PGMA layer with quite low molecular weights (6 600 and 12 500 g·mol^{-1}) almost did not affect magnetic susceptibility. Therefore, the MR suspension containing modified CI particles is able to interact with an external magnetic

field comparably to the suspension of bare CI particles, which was reflected in the almost unaffected values of viscoelastic moduli of prepared MR suspensions. Decreased values of G' in the off-state for modified MR suspensions ultimately led to higher values of dynamic efficiency.

3.8 Sedimentation stability

Figure 10 shows the weight gain representing settling particles as a function of observation time. On the basis of the graphed results, it can be confidently asserted that the use of core-shell CI-PGMA particles as a dispersed phase considerably enhanced the sedimentation stability of MR suspensions compared to suspension of the same amount of bare CI particles. Improved sedimentation stability of suspensions containing CI-PGMA particles is due to the presence of PGMA polymer chains which contribute to the reduced bulk density of composite particles [1, 2] and provide better compatibility with silicone oil [38]. The suspension based on CI-PGMA-2 particles exhibits only a slight improvement in sedimentation stability compared to the suspension based on CI-PGMA-1, thus the length of polymer chains does not play that important of a role as expected. The probe entrapping settling particles was placed close to the surface, therefore the phase interface passed through this area after a while; hence the weight gain quickly reached its asymptotic value. Thus, this method provided fast estimation of sedimentation velocity.

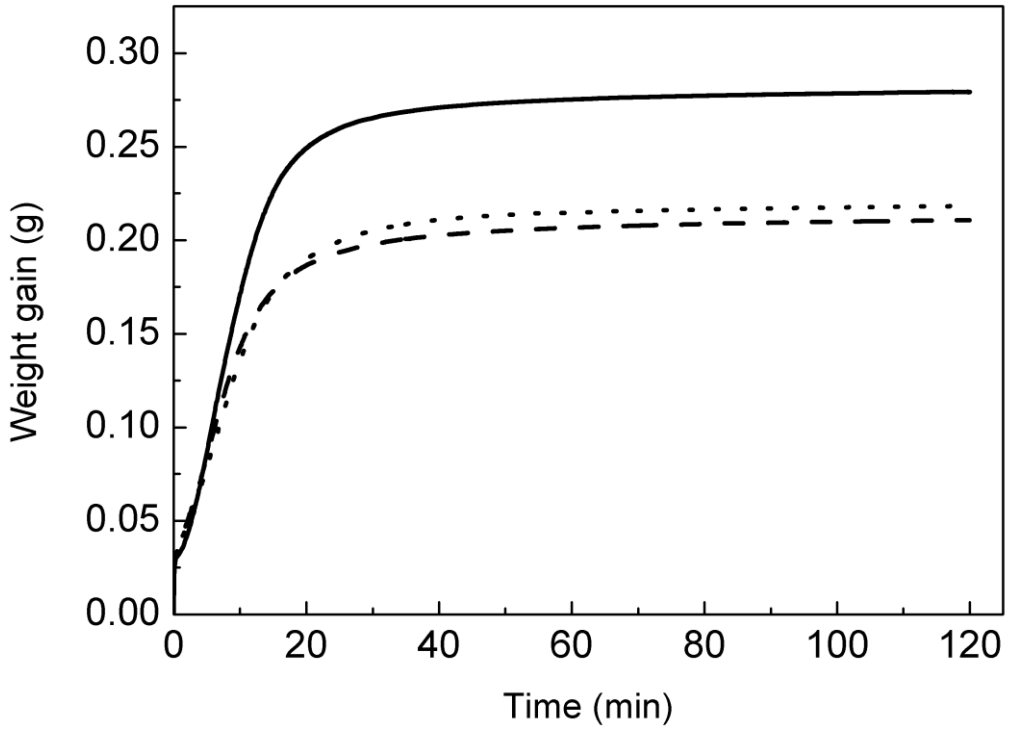

Figure 10. Time dependence of the weight gain representing settled particles for 10 wt.% MR suspensions based on bare CI particles (–), CI-PGMA-1 particles (····), and CI-PGMA-2 particles (- - -) in silicone oil.

4. Conclusion.

The surface of CI particles was controllably coated with PGMA in order to enhance thermo-oxidation and sedimentation stability while maintaining their sufficient magnetic properties. These aims were fulfilled with the use of CI-PGMA particles prepared *via* facile SI-ATRP. Two types of core-shell particles were synthesized, in which the polymer shell consisted of PGMA with molecular weights of either 6,600 $g \cdot mol^{-1}$ or 12,500 $g \cdot mol^{-1}$ PDI of 1.32 and 1.29, respectively. The presence of the PGMA shell was proved by EDS and FTIR spectroscopies. A

slight decrease in magnetization was detected due to the non-magnetic coating, which was measured at 780 $kA \cdot m^{-1}$ as a 3.9 % decrease for CI-PGMA-1 particles and a 5.3 % decrease for CI-PGMA-2 particles. Surface modification with PGMA further considerably enhanced thermo-oxidation stability and shifted the oxidation of the particles towards higher temperatures about more than 100 °C. However, doubling the molecular weight of PGMA contributed to only a slight improvement.

Furthermore, the viscoelastic properties of MR suspensions were investigated at various magnetic field strengths. MR suspensions of 60 wt.% particles exhibited promising values of G' and G'', and these remained almost on the same level for MR suspensions of PGMA-coated particles due to negligibly-decreased magnetic susceptibility. Moreover, sedimentation stability was significantly enhanced due to reduced bulk density and the presence of the PGMA polymer chains on the particle surface providing better interactions with silicone oil. Therefore, it can be concluded that the SI-ATRP method was favorably utilized as an effective tool for defined modification of particles used in MR suspensions with tunable MR performance and stability properties.

AUTHOR INFORMATION

Corresponding Author

* Miroslav Mrlik, mrlik@ft.utb.cz

Author Contributions

The manuscript was contributed to by the listed authors, all of whom have approved of its final form.

ACKNOWLEDGMENTS

The authors M. C. and T. P. further thank the internal grant of TBU in Zlin No. IGA/FT/2014/017, funded from specific university research resources. Author M. S. wishes to thank the Grant Agency of the Czech Republic (14-32114P) for financial support. This article was written with support of the Operational Program Research and Development for Innovations co-funded by the European Regional Development Fund (ERDF) and the National Budget of Czech Republic, within the framework of the project Centre of Polymer Systems (CZ.1.05/2.1.00/03.0111). J. M. and M. I. thank the Centre of Excellence FUN-MAT for financial support.

REFERENCES

[1] de Vicente, J.; Klingenberg, D. J.; Hidalgo-Alvarez, R. Magnetorheological fluids: a review. *Soft Matter*. **2011**, *7*, 3701–3710.

[2] Park, B. J.; Fang, F. F.; Choi, H. J. Magnetorheology: materials and application. *Soft Matter*. **2010**, *6*, 5246–5253.

[3] Sedlacik, M.; Pavlinek, V.; Saha, P.; Svrcinova, P.; Stejskal, J. Rheological properties of magnetorheological suspensions based on core-shell structured polyaniline-coated carbonyl iron particles. *Smart Materials and Structures*. **2010**, *19*, 115008.

[4] Kim, S. Y.; Kwon, S. H.; Liu, Y. D.; Lee, J. S.; You, Ch. Y. Core-shell-structured cross-linked poly(glycidyl methacrylate)-coated carbonyl iron microspheres and their magnetorheology. *Journal of Materials Science*. **2014**, *49*, 1345–1352.

[5] Liu, Y. D.; Choi, H. J. Recent progress in smart polymer composite particles in electric and magnetic fields. *Polymer International*. **2013**, *62*, 147–151.

[6] Sedlacik, M.; Pavlinek, V.; Peer, P.; Filip, P. Tailoring the magnetic properties and magnetorheological behavior of spinel nanocrystalline cobalt ferrite by varying annealing temperature. *Dalton Transactions*. **2014**, *43*, 6919–6924.

[7] Yu, M.; Dong, X. M.; Choi, S. B.; Liao, C. R. Human simulated intelligent control of vehicle suspension system with MR dampers. *Journal of Sound and Vibration.* **2009**, *319*, 753–767.

[8] Atabay E.; Ozkol I. Application of a magnetorheological damper modeled using current-dependent Bouc-Wen model for shimmy suppression in a torsional nose landing gear with and without freeplay, *Journal of Vibration and Control.* **2014**, *20*, 1622–1644.

[9] Ha, Q. P.; Nguyen, M. T.; Li, J.; Kwok, N. M. Smart structures with current-driven MR dampers: modeling and second-order sliding mode control. *IEEE/ASME Transactions on Mechatronics*. **2013**, *18*, 1702–1712.

[10] Chen, Z. Q.; Wang, X. Y.; Ko, J. M.; Ni, Y. Q.; Spencer, B. F.; Yang, G.; Liu, S. Ch. MR damping system on Donting Lake cable-stayed bridge. *Smart Structures and Materials.* **2003**, *5057*, 229–235.

[11] Karakoc, K.; Park, J. E.; Suleman, A. Design considerations for an automotive magnetorheological brake. *Mechatronics.* **2008**, *18*, 434–447.

[12] Wang, D. M.; Hou, Y. F.; Tian, Z. A novel high-torque magnetorheological brake with a water cooling method for heat dissipation. *Smart Materials and Structures*. **2013**, *22,* 025019.

[13] Rabinow, J. The magnetic fluid clutch. *AIEE Trans*., **1948**, *67*, 1308–1315.

[14] Kavlicoglu, B. M.; Gordaninejad, F.; Wang, X. Study of a magnetorheological grease clutch. *Smart Materials and Structures*. **2013**, *22*, 125030.

[15] Herr, H.; Wilkenfeld, A.; Huseyin, S.; Gordaninejad, F.; Evrensel, C. User-adaptive control of a magnetorheological prosthetic knee. *Industrial Robot: An International Journal*. **2003**, *30*, 42–55.

[16] Jang, K. I.; Seok, J.; Min, B. K.; Lee, S. J. An electrochemomechanical polishing process using magnetorheological fluid. *International Journal of Machine Tools and Manufacture*. **2010**, *50*, 869–881.

[17] Silva, A. A.; Silva, E.; Carrico, A.; Egito, E. T. Magnetic carriers: a promising device for targeting drugs into the human body. *Current Pharmaceutical Design*. **2007**, *13*, 1179–1185.

[18] Flores, G. A.; Sheng, R.; Liu, J.; Lee, S. J. Medical applications of magnetorheological fluids a possible new cancer therapy. *Journal of Intelligent Material Systems and Structures*. **2001**, *10*, 708–713.

[19] Phule, P. P.; Ginder, J. M. Synthesis and properties of novel magnetorheological fluids having improved stability and redispersibility. *International Journal of Modern Physics*. **1999**, *13*, 2019–2027.

[20] Lopez-Lopez, M. T.; Zugaldia, A.; Gonzalez-Caballero, F.; Duran, J. D. G. Sedimentation and redispersion phenomena in iron-based magnetorheological fluids. *Journal of Rheology*. **2006**, *50*, 543–560.

[21] Alves, S.; Alcantara, M. R.; Figueiredo-Neto, A.M.; Duran, J. D. G. The effect of hydrophobic and hydrophilic fumed silica on the rheology of magnetorheological suspensions. *Journal of Rheology*. **2009**, *53*, 651–662.

[22] Lim, S. T.; Choi, H. J.; Jhon, M. S. Magnetorheological characterization of carbonyl iron-organoclay suspensions. *IEEE Transactions on Magnetics*. **2005**, *41*, 3745–3747.

[23] Pu, H. T.; Jiang, F. J.; Yang, Z.; Yan, B.; Liao, X. Effects of polyvinylpyrrolidone and carbon nanotubes on magnetorheological properties of iron-based magnetorheological fluids. *Journal of Applied Polymer Science*. **2006**, *102*, 1653–1657.

[24] Bica, I.; Jiang, F. J.; Yang, Z.; Yan, B.; Liao, X. Magnetorheological suspension based on mineral oil, iron and graphite micro-particles. *Journal of Magnetism and Magnetic Materials*. **2004**, *283*, 335–343.

[25] Hu, B.; Fuchs, A.; Huseyin, S.; Gordaninejad, F.; Evrensel, C. Atom transfer radical polymerized MR fluids. *Polymer*. **2006**, *47*, 7653–7663.

[26] Choi, H. J.; Park, B. J.; Cho, M. S.; You, J. L. Core-shell structured poly(methyl methacrylate) coated carbonyl iron particles and their magnetorheological characteristics. *Journal of Magnetism and Magnetic Materials*. **2007**, *310*, 2835–2837.

[27] Quan, X.; Chuah, W.; Seo, Y.; Choi, H. J. Core-shell structured polystyrene coated carbonyl iron microspheres and their magnetorheology. *IEEE Transactions on Magnetics*. **2014**, *50*, 1–4.

[28] Jang, I.B.; Kim, H. B.; Lee, J. Y.; You, J.L.; Choi, H.J.; Jhon, M. S. Role of organic coating on carbonyl iron suspended particles in magnetorheological fluids. *Journal of Applied Physics.* **2005**, *97*, 10Q912.

[29] Fang, F. F.; Liu, Y. D.; Choi, H. J. Fabrication of carbonyl iron embedded polycarbonate composite particles and magnetorheological characterization. *IEEE Transactions on Magnetics*. **2009**, *45*, 2507–2510.

[30] Sedlacik, M.; Pavlinek, V.; Lehocky, M.; Mracek, A.; Grulich, O.; Svrcinova, P.; Filip, P.; Vesel, A. Plasma-treated carbonyl iron particles as a dispersed phase in magnetorheological fluids. *Colloids and Surfaces A: Physicochemical and Engineering Aspects*. **2011**, *387*, 99–103.

[31] Mrlik, M.; Sedlacik, M.; Pavlinek, V.; Bazant, P.; Saha, P.; Peer, P.; Filip, P. Synthesis and magnetorheological characteristics of ribbon-like, polypyrrole-coated carbonyl iron suspensions under oscillatory shear. *Journal of Applied Polymer Science*. **2013**, *128*, 2977–2982.

[32] Wang, J. S.; Matyjaszewski, K. Controlled living polymerization - atom-transfer radical polymerization in the presence of transition-metal complexes. *Journal of the Americal Chemical Society*. **1995**, *117*, 5614–5615.

[33] Matyjaszewski, K.; Chuah, W.; Seo, Y.; Choi, H. J. Atom Transfer Radical Polymerization (ATRP): Current Status and Future Perspectives. *Macromolecules.* **2012**, *45*, 4015–4039.

[34] Sutrisno, J.; Fuchs, A.; Sahin, H.; Gordaninejad, F. Surface coated iron particles via atom transfer radical polymerization for thermal-oxidatively stable high viscosity magnetorheological fluid. *Journal of Applied Polymer Science*. **2013**, *128*, 470–480.

[35] Mosnacek, J.; Ilcikova, M. Photochemically mediated atom transfer radical polymerization of methyl methacrylate using ppm amounts of catalyst. *Macromolecules*. **2012**, *45*, 5859–5865.

[36] Belyavskii, S. G.; Mingalyov, P. G.; Giulieri, F.; Combarrieau, R.; Lisichkin, G. V. Chemical modification of the surface of a carbonyl iron powder. *Protection of Metals*. **2006**, *42*, 244–252.

[37] Mrlik, M.; Ilcikova, M.; Pavlinek, V.; Mosnacek, J.; Peer, P.; Filip, P. Improved thermooxidation and sedimentation stability of covalently-coated carbonyl iron particles with cholesteryl groups and their influence on magnetorheology. *Journal of Colloid and Interface Science*. **2013**, *396*, 146–151.

[38] Sedlacik, M.; Pavlinek, V. A tensiometric study of magnetorheological suspensions´ stability. *RSC Advances*. **2014**, *4*, 58377–58385.

[39] Wang, W. C.; Zhang, Q.; Zhang, B. B.; Li, D. N.; Dong, X. Q.; Zhang, L.; Chang, J. Preparation of monodisperse, superparamagnetic, luminescent, and multifunctional PGMA microspheres with amino-groups. *Chinese Science Bulletin*. **2008**, *53*, 1165–1170.

[40] Zhao, R.; Lu, J.; Tan, T. Preparation of polyglycidylmethacrylate macropore beads and application in *Candidaspecies 99-125* lipase immobilization. *Chemical Engineering*. **2011**, *34*, 93–97.

[41] de Vicente, J.; Bossis, G.; Lacis, S.; Guyot, M. Permeability measurements in cobalt ferrite and carbonyl iron powders and suspensions. *Journal of Magnetism and Magnetic Materials*. **2002**, *251*, 100–108.

[42] Abshinova, M. A.; Kazantseva, N. E.; Saha, P.; Sapurina, I.; Kovarova, J.; Stejskal, J. The enhancement of the oxidation resistance of carbonyl iron by polyaniline coating and consequent changes in electromagnetic properties. *Polymer Degradation and Stability*. **2008**, *93*, 1826–1831.

[43] Claracq, J.; Sarrazin, J.; Montfort, J. P. Viscoelastic properties of magnetorheological fluids. *Rheologica Acta*. **2004**, *43*, 38–49.

[44] Ramos, J.; de Vicente, J.; Hidalgo-Alvarez, R. Small-amplitude oscillatory shear magnetorheology of inverse ferrofluids. *Langmuir*. **2010**, *26*, 9334–9341.